Received: 16 August 2021 | Accepted: 27 October 2021

DOI: 10.1111/iej.13655

INTERNATIONAL ENDODONTIC JOURNAL | WILEY

ORIGINAL ARTICLE

Chronic apical periodontitis exacerbates atherosclerosis in apolipoprotein E-deficient mice and leads to changes in the diversity of gut microbiota

Guowu Gan[1,2] | **Beibei Lu**[1,2] | **Ren Zhang**[1,2] | **Yufang Luo**[1,2] | **Shuai Chen**[1,2] | **Huaxiang Lei**[1,2] | **Yijun Li**[1,2] | **Zhiyu Cai**[3] | **Xiaojing Huang**[1,2]

[1]Fujian Key Laboratory of Oral Diseases & Fujian Provincial Engineering Research Center of Oral Biomaterial & Stomatological Key lab of Fujian College and University, School and Hospital of Stomatology, Fujian Medical University, Fuzhou, China

[2]Institute of Stomatology, Research Center of Dental and Craniofacial Implants, School and Hospital of Stomatology, Fujian Medical University, Fuzhou, China

[3]Department of Stomatology, Fujian Medical University Union Hospital, Fuzhou, China

Correspondence
Xiaojing Huang, School and Hospital of Stomatology, Fujian Medical University, Fuzhou 350002, China.
Emails: hxiaoj@163.com, xiaojinghuang@fjmu.edu.cn

Funding information
This work was supported by the National Natural Science Foundation of China (grant nos. 81970926, 81500845).

Abstract

Aim: To investigate the impact of chronic apical periodontitis (CAP) on atherosclerosis and gut microbiota by establishing a *Porphyromonas gingivalis* (*P. gingivalis*)-induced CAP in an apolipoprotein E-deficient (apoE$^{-/-}$) mice model.

Methodology: Twenty-eight male apoE$^{-/-}$ mice were divided into two groups with 14 in each: CAP group and control group. In the CAP group, sterile cotton wool containing 10^8 colony-forming units of *P. gingivalis* was placed into the pulp chamber after pulp exposure followed by coronal resin filling in bilateral maxillary first and second molars. The mice were fed with a chow diet to induce atherosclerosis. Animals were euthanized 16 weeks after the operation, and the periapical lesions of bilateral maxillary first and second molars were assessed by micro-CT. After collection of aortic arches, atherosclerotic lesions were measured by Oil Red O staining. Serum levels of high-density lipoprotein cholesterol (HDL-C), low-density lipoprotein cholesterol (LDL-C), total cholesterol (TC), and triglycerides (TG) were measured. Stools were collected to detect alterations in gut microbiota by 16S rRNA gene sequencing. Independent samples *t*-test was used to calculate the difference between the two groups.

Results: CAP was observed in 98.2% of molars. A significant increase in atherosclerotic plaque formation in the aortic arches was found in the CAP groups (CAP: 2.001% ± 0.27%, control: 0.927% ± 0.22%, $p = .005$). No significant difference was observed between sevum level of HDL-C (CAP: 2.295 ± 0.31 mmol/L, Control: 3.037 ± 0.55 mmol/L, $p = .264$) or LDL-C (CAP: 17.066 ± 3.95 mmol/L, Control: 10.948 ± 1.69 mmol/L, $p = .177$) in CAP group and Control group. There were no significant differences in TG (CAP: 1.076 ± 0.08 mmol/L, control: 1.034 ± 0.13 mmol/L, $p = .794$) or TC (CAP: 6.372 ± 0.98 mmol/L, control: 6.679 ± 0.75 mmol/L, $p = .72$) levels between the two groups ($p > .05$). The alpha diversity was elevated in the CAP group. In terms of beta diversity, the CAP and control groups were clearly distinguished by the microbial community.

Guowu Gan and Beibei Lu contributed equally to this study.

Conclusion: In a mouse experimental model, pulp infection with *P. gingivalis* -induced CAP, thus aggravating the development of atherosclerosis. Meanwhile, CAP increased alpha diversity and altered the beta diversity of the gut microbiota.

KEYWORDS

animal model, atherosclerosis, chronic apical periodontitis, gut microbiota, *Porphyromonas gingivalis*

INTRODUCTION

Cardiovascular disease (CVD) is the main cause of death worldwide (Tymchuk et al., 2006) and encompasses many risk factors, such as hypertension, diabetes and chronic inflammation. The major risk factor for CVD is atherosclerosis, which is characterized by a slow accumulation of lipid-laden plaques and macrophages in medium- and large-sized arteries (Gistera & Hansson, 2017). Of note, a substantial proportion of atherosclerotic patients do not have significant hyperlipidaemia (Shapiro & Fazio, 2016). Infection may contribute to the development of atherosclerosis. Interventions that regulate systemic or local inflammatory responses have become attractive means to lower the risk of CVD (Shapiro & Fazio, 2016). It may be the direct effect of infecting vascular cells and/or the indirect effect of cytokines and acute-phase reactive proteins caused by an infection in other sites (Campbell & Rosenfeld, 2015). Oral pathogens have been identified in atherosclerotic plaques, including *Prevotella intermedia*, *Tannerella forsythia* and *Porphyromonas gingivalis* (Aimetti et al., 2007). Chronic apical periodontitis (CAP) is considered a potential risk for systemic diseases, including CVD (Bui et al., 2019; Segura-Egea et al., 2015).

CAP is an inflammatory response of periapical tissue to an infected root canal system. The infected root canal and the host's immune response cause the removal of calcified periapical tissue (Persoon & Ozok, 2017). This infection is similar to periodontal disease and Gram-negative anaerobes play an important role (Berlin-Broner et al., 2017). *P. gingivalis*, a Gram-negative anaerobe that is involved in infecting the pulp chamber in apical periodontitis, has been reported to be closely correlated with the development of atherosclerosis (Gibson et al., 2004). CAP can be detected radiographically as a radiolucent lesion in the surrounding alveolar bone adjacent to the apex of the infected tooth, which is very common and occurs in 34% of patients (Lopez-Lopez et al., 2012). Given that periapical lesions are usually painless, that may not be detected for many years and it may become chronic (Sullivan et al., 2016; Yu et al., 2012). More and more evidence indicates that CAP may not be restricted locally (Zhang et al., 2016). A retrospective evaluation of the CT scans of 531 patients reported that CAP was positively correlated with atherosclerotic lesions (Petersen et al., 2014). The number of teeth affected by CAP is significantly associated with cardiovascular events (Gonzalez-Navarro et al., 2020). In a cross-sectional study that included 120 men between the ages of 20 and 40 who did not have CVD, periodontal disease, traditional cardiovascular risk factors and impaired flow-mediated dilatation, elevated carotid intima-media thickness was found in subjects with CAP, which indicates a possible association between dental pulp infection and CVD (Chauhan et al., 2019). A logistic regression model revealed a significant positive correlation between CAP and CVD (odds ratio, 5.3; An et al., 2016). CAP can also affect total cholesterol (TC) levels and influences the increase in carotid endothelial thickness in the presence of atherosclerosis (Conti et al., 2020).

Although many epidemiological studies have reported a connection between CAP and CVD, the causal relationship between CAP and atherosclerosis has not been confirmed (Jimenez-Sanchez et al., 2020). The difficulty of controlling potential confounding factors and the complexity of systemic disease make it challenging to conduct longitudinal studies in humans to confirm causality. Meanwhile, animal experiments are advantageous in providing data to support the causal relationship between CAP and atherosclerosis. The lack of animal studies may be due to the complexity of microsurgical techniques and the long experimental period (Berlin-Broner et al., 2020). In a previous study, the pulp cavity of C57BL/6J mice was infected with *P. gingivalis*, and mice in the high-fat diet group had *P. gingivalis* bacteria in the arterial smooth muscle and had endothelial damage in arteries; however, typical atherosclerotic plaques were not detected (Ao et al., 2014). Recently, in a CAP model induced in LDLr knockout ($LDLr^{-/-}$) mice, the pulp cavities of four first molars were opened, the percentage of periapical lesions (PALs) found in all four molars was 27.7%, and the degree of atherosclerosis was similar in the CAP and Control groups (Berlin-Broner et al., 2020). Combining induction of CAP by of *P. gingivalis* dental infection and genetically engineered mouse models of atherosclerosis is a new approach to investigate the causal relationship between CAP and atherosclerosis.

The gut microbiota consists of trillions of microorganisms that play an important role in dietary energy

harvesting. More and more evidences suggest that alterations in the gut microbiota and its metabolites exacerbate the development of atherosclerosis (Koeth et al., 2013; Tang et al., 2013; Wang et al., 2011). Proinflammatory flora can increase systemic inflammation in Ldlr$^{-/-}$ mice and accelerate the formation of atherosclerosis (Brandsma et al., 2019). In apolipoprotein E-deficient (apoE$^{-/-}$) mice with *P. gingivalis*-induced periodontitis, the degree of atherosclerosis is aggravated (Suh et al., 2019). Bacteria from the mouth or gut may be associated with disease markers of atherosclerosis (Koren et al., 2011). However, few studies have investigated the role of gut microbiota in the relationship between CAP and atherosclerosis.

Therefore, it was hypothesized that *P. gingivalis*-induced CAP could alter the composition and diversity of gut microbiota and exacerbate atherosclerosis. To testify this, in the present study, a *P. gingivalis*-nduced CAP apoE$^{-/-}$ mouse model was established. Atherosclerotic lesions of aortic arches, serum levels of high-density lipoprotein cholesterol (HDL-C), low-density lipoprotein cholesterol (LDL-C), TC, and triglycerides (TG) were measured. Alteration in gut microbiota was detected by 16S rRNA gene sequencing.

MATERIALS AND METHODS

Mice and operation

Care and handling of laboratory animals followed the guidelines of the Laboratory Animal Care Institute of Fujian Medical University. The Animal Care and Use Committee of Fujian Medical University approved all animal procedures before the start of the study (protocol number 2020-0041). The experiments were conducted in compliance with Preferred Reporting Items for Animal Studies in Endodontology (PRIASE) guidelines (Nagendrababu et al., 2021). The sample size was calculated referring to a power calculation from a previous study using G*power version 3.1.9.7 (https://stats.idre.ucla.edu/other/gpower/, UCLA, USA). The sample size was 12 mice per group in order to achieve a p-value <.05 with 80% power. Considering the long period of the study and establishment of the CAP model, the number of mice was increased to 14 in each group. This sample size also complied with the recommendation of the American Heart Association (Daugherty et al., 2017). The qualifications of animal caretakers met the requirements (Fujian Laboratory Animal Committee No. 2019-0080). The mice were kept in a specific pathogen-free environment with a 12-h light/dark cycle and had free access to food and water. Twenty-eight 5-week-old male mice (Cyagen Biological Technology Co., Ltd.) were randomly divided into two groups after 1 week of acclimatization and fed a chow diet (Beijing Keao Xieli Feed Co., Ltd.) to induce atherosclerosis. The root canals of bilateral first and second molar of mice in the CAP group were infected with *P. gingivalis* after pulp chamber exposure under anaesthesia, whilst those in the control group were only anaesthetized without further operation, both groups waked up in a warm blanket after anaesthesia. In the CAP group, intramuscular injection of pethidine (2 mg kg^{-1}) was used to minimize pain. In all operations, mice were anesthetized by 1% sodium pentobarbital (0.1 ml/10 g; Sigma-Aldrich) by intramuscular injection. A FG 1/4 round bur (Dianfeng Abrasive Materials Co., Ltd.) was used to expose the pulp cavity of the bilateral maxillary first molars, and a Tc-21EF needle shape diamond bur (Haixiang Medical Equipment Co., Ltd.) was used for bilateral maxillary second molars (Figure 1a–b). After opening the pulp cavity, a small piece of sterile cotton wool, containing 0.2 μl of 10^8 colony-forming units (CFU) of *P. gingivalis* (ATCC33277 strain), was inserted into the pulp cavity.

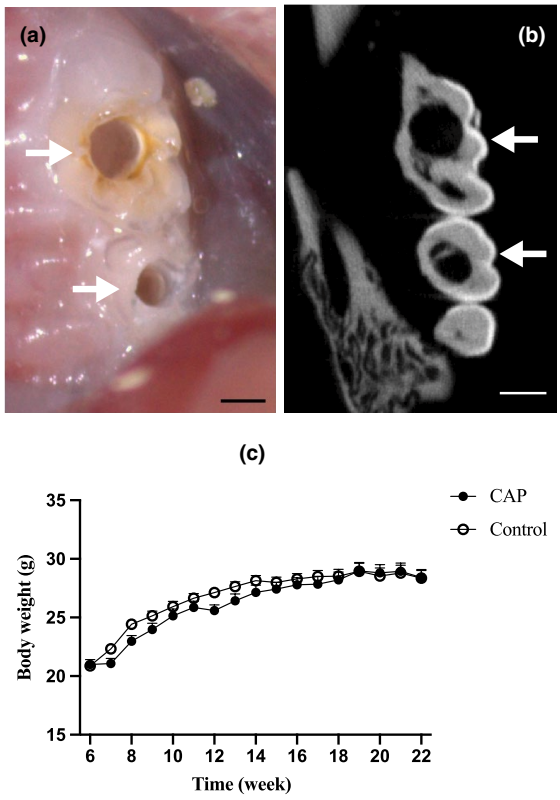

FIGURE 1 The left maxillary first and second molars in the CAP group under stereomicroscope (a) and micro-CT (b) (scale bar: 500 μm). The white arrow indicates the pulp exposure site. No significant difference was observed in the body weight at different time points between CAP and control group (c). ($p > .05$).

After etching and bonding, the cavity was sealed with flowable resin (3 M, Sao Paulo, Minnesota, USA).

Bacterial culture

In an anaerobic chamber (YAX-II anaerobic chamber, Shanghai Xinmiao Medical Equipment Manufacture Co., Ltd), the *P. gingivalis* strain ATCC33277 was cultured in Brian Heart Infusion medium at 37°C for 48 h. Bacterial suspensions were prepared in phosphate-buffered saline using an established standard curve and spectral analysis. The number of CFUs was normalized by measuring the optical density (OD; 630 nm). It was determined that an OD of 1 was equal to 10^8 CFU.

Micro-CT analysis

After euthanasia by an overdose of anaesthesia 16 weeks after surgery, the heads of the mice were collected, the bilateral maxillae were excised, and the soft tissues were removed, fixed in 4% neutral paraformaldehyde for 24 h, and preserved in 70% ethanol. Micro-CT scans of mouse maxillary tissues were taken at 15 μm. Images were scanned with a resolution of 1024*1024 and a pixel ruler of 15*15 μm (μCT100, Seanco Medical). The samples were placed in a test tube and scanned along the axis. Mimics software (Materialise) was used to reconstruct the periapical bone resorption region. Two dentists who were blinded to the experiment evaluated the results of micro-CT and counted teeth with PALs.

Staining and quantification of atherosclerotic lesions in aortic arch

The aortic arch was opened along the inward and outward bends under a stereomicroscope (Leica Camera AG). In atherosclerotic lesions analysis, the aortic arch was stained with Oil Red O (Sigma-Aldrich) as previously described (Centa et al., 2019). Aortic arch images were captured with a stereoscopic microscope and analysed using ImageJ (NIH; http://imagej.nih.gov/ij). Two researchers who were blind to the experiment independently used the image-Adjust-Colour threshold function in ImageJ to count the plaque area with the same parameters and used the wand tool to select the overall area of the aortic arch. The percentage of lesion area was calculated as the total lesion area divided by the total area of the aortic arch. An average value was obtained after repeating it three times. Inter-rater reliability between the two observes was obtained (>0.90). In the formal study, the value of each sample was obtained by calculating the average of the measurements by the two researchers.

Serum lipid evaluation

At 16 weeks post-surgery, mice were operated under anaesthesia. Blood was collected after removal of the eyeball, and then stored at room temperature for 2 h for serum separation. After centrifugation at 4°C and 1000 g for 10 min, serum was extracted and stored at −80°C for freezing. HDL-C, LDL-C, TC, and TG were measured using a kit (Nanjing Jiancheng Institute of Biological Engineering Co., Ltd.).

Microbiota DNA sequencing

Fresh faecal samples from the mice were collected 16 weeks after treatment. The samples were placed into containers with dry ice during transportation and stored at −80°C in 10 min. The total DNA was extracted according to the instructions of the EZNA® soil kit (Omega Bio-Tek). The quantity and quality of the extracted DNA were measured using a NanoDrop ND-2000 UV-Vis spectrophotometer (Thermo Fisher Scientific) and agarose gel electrophoresis. PCR amplification of the V3–V4 variable region was conducted with the following primers: 338F (5′-ACTCCTACGGGAGGCAGCAG-3′) and 806R (5′-GGACTACHVGGGTWTCTAAT-3′) primers. The amplification procedure was as follows: 95℃ predenaturation for 3 min, 27 cycles (95°C denaturation for 30 s, 55°C annealing for 30 s, 72°C extension for 30 s), and finally 72°C extensions for 10 min (PCR instrument: ABI GeneAmp®). The amplification system comprised 20 μl:4 μl of 5*FastPfu buffer, 2 μl of 2.5 mmol L^{-1} dNTPs, 0.8 μl of primer (5 μmol L^{-1}), 0.4 μl of FastPfu polymerase and10 ng of DNA template. PCR products were extracted from 2% agarose gels and extracted using the AxyPrep DNA Gel Extraction Kit (Axygen Biosciences) for further purification and quantification using QuantiFluor™-ST (Promega) according to the manufacturer's protocol. After a separate quantification step, the purified amplicons were pooled in equimolar and double-end sequencing (2 × 300) on an Illumina MiSeq platform (Illumina) according to standard protocols.

Bioinformatic analysis

The analysis was performed using QIIME2 (https://docs.qiime2.org/2019.1/). Briefly, raw data FASTQ raw data

files were imported into the format that could be operated by the QIIME2 system using Qiime tools import program. Demultiplexed sequences from each sample were quality filtered and trimmed, de-noised and merged. Then, the chimeric sequences were identified and removed using the QIIME2 DADA2 plugin to obtain the feature table of amplicon sequence variant (ASV; Callahan et al., 2016). Next, the QIIME2 feature-classifier plugin was applied to match the representative sequences of ASV to the pre-trained version 13_8, 99% similarity GREENGENES database (the database was pruned to the region of V3–V4 on the basis of 338F/806R primer pairs), and the matching threshold was set to 70% to obtain the taxonomic information table of species (Bokulich et al., 2018). Any contaminating mitochondrial and chloroplast sequences were filtered using the QIIME2 feature-table plugin. Appropriate methods including analysis of composition of microbiomes (ANCOM), analysis of variance (ANOVA), Kruskal–Wallis, linear discriminant analysis effect size (LEfSe), and DEseq2 were employed to identify bacteria with different abundance amongst samples and groups (Love et al., 2014; Mandal et al., 2015; Segata et al., 2011). Diversity metrics were calculated using the core-diversity plugin within QIIME2. Feature level alpha diversity indices, such as observed operational taxonomic units (OTUs), Chao1 richness estimator, Shannon diversity index, and Faith's phylogenetic diversity index, were calculated to estimate the microbial diversity within an individual sample. The beta diversity distance measurements, including Bray–Curtis, unweighted UniFrac, and weighted UniFrac, were performed to investigate the structural variation of microbial communities across samples and then visualized via principal coordinate analysis (PCoA) and nonmetric multidimensional scaling (Vazquez-Baeza et al., 2013). Applying the R package 'vegan', the redundancy analysis approach was used to reveal potential associations between microbial communities and relevant environmental factors. Co-occurrence analysis was performed by calculating Spearman's rank correlations between predominant taxa and the network plot was used to display the associations amongst taxa. Unless specified above, parameters used in the analysis were set as default.

Data analysis

Graphs were created and statistical analyses were calculated using GraphPad Prism 9 (GraphPad Prism software, San Diego, CA, USA). For comparison of the two groups, independent samples *t*-test was used after determining data normality and homogeneity of variance test. A *p*-value of less than .05 was considered significant. Error bars represent mean ± SEM.

RESULTS

Evaluation of the physical condition of apoE$^{-/-}$ mice after dental infection of *P. gingivalis*

No significant difference was observed in the body weight at different time points (0, 2, 4, 6, 8, 10, 12, 14, 16 weeks after operation) between CAP and control group (Figure 1c; $p > .05$). At the 16 week time point, the average weight and weight gain percentage in the CAP group was: 28.40 ± 0.61 g, 35.62% ± 2.69%, whilst those in the control group was 28.35 ± 0.73 g, and 36.20% ± 3.91%, respectively ($p > .05$).

Micro-CT evaluation of the apical region after dental infection of *P. gingivalis*

The micro-CT scan confirmed that, except for the second molar of one mouse, PALs were found in the rest of the teeth. A representative micro-CT image and matching tissue section are shown in Figure 2a–b.

Percentage increase in atherosclerotic lesion area in apoE$^{-/-}$ mice after dental infection of *P. gingivalis*

To clarify whether CAP can exacerbate atherosclerosis, the protocol for detecting lesions at the aortic arch was referenced using Oil Red O staining with a chow diet was used (Centa et al., 2019). The percentage of lesion area at the aortic arch was significantly increased in the CAP group compared with the Control group (CAP: 2.001% ± 0.27%, Control: 0.927% ± 0.22%, $p = .005$) (Figure 3a–b).

Assessment of serum lipids after dental infection of *P. gingivalis* in apoE$^{-/-}$ mice

The results of serum lipid profiles (HDL-C, LDL-C, TC, TG) are shown in Figure 4a–d. The level of HDL-C was decreased (CAP: 2.382 ± 0.25 mmol/L, Control: 3.171 ± 0.44 mmol/L, $p = .126$) in the CAP group, and the level of LDL-C was increased (CAP: 17.066 ± 3.95 mmol/L, Control: 10.948 ± 1.69 mmol/L, $p = .177$). However, the difference was not significant ($p > .05$). The changes in TG (CAP: 1.076 ± 0.08 mmol/L, Control: 1.034 ± 0.13 mmol/L, $p = .794$) and TC (CAP: 6.372 ± 0.98 mmol/L, Control: 6.679 ± 0.75 mmol/L,

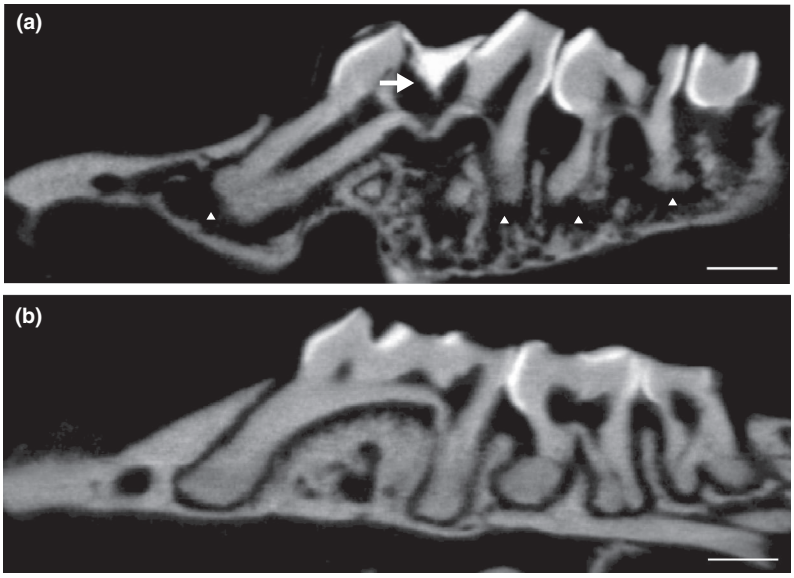

FIGURE 2 Sagittal sections of the micro-CT images of the left maxillary first and second molars in the CAP (a) and control (b) groups (scale bar: 500 μm). The white triangle indicates periapical lesions (PALs).

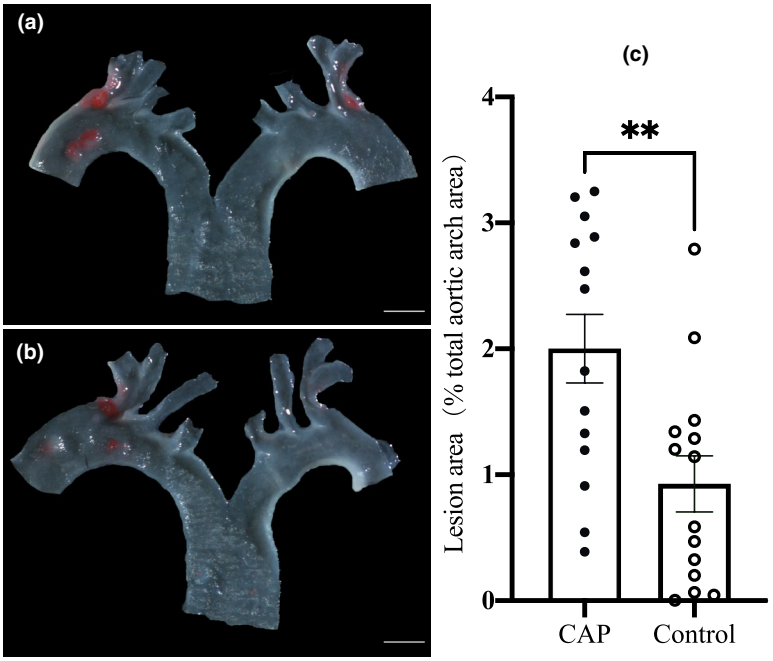

FIGURE 3 *P. gingivalis* induced CAP increased plaque formation in the aortic arch. Oil Red O-stained aortic arches from mice in the CAP (a) and the control (b) group (scale bar: 1 mm). A significantly higher percentage of Oil Red O-stained area of aortic arches was observed in the CAP group than the control group ($n = 14$ in each group) (c). (** means $p < .01$).

$p = .72$) levels were similar in both groups and not significant ($p > .05$).

Dental infection of *P. gingivalis* in apoE$^{-/-}$ mice alters gut microbiota composition

After 16 weeks of dental infection with *P. gingivalis*, the fresh stool was collected for the 16S rRNA gene sequence to define the microbiota composition. At the genus level, the proportions of *Allobaculum*, and *Sutterella were* elevated, whilst those of *Lactobacillus* and *Helicobacter* were lower in the CAP group than in the Control group (Figure 5a). LEfSe was applied to the microbiota data of both groups and identified 37 differentially abundant taxa (alpha = 0.05) with an LDA score higher than 2.0, respectively (Figure 5b). At the genus level, *Akkermansia* was the most abundant in the CAP group, whilst *Ruminococcus* was the most abundant in the Control group (Figure 5b). The Faith's phylogenetic diversity, Shannon index, and Simpson index of the CAP group were higher than those of the Control group, and the Shannon index ($p = .052$). The difference between Faith's phylogenetic diversity and Simpson index was significant, with $p < .01$ (Figure 6a–c). Beta diversity analysis compared bacterial communities according

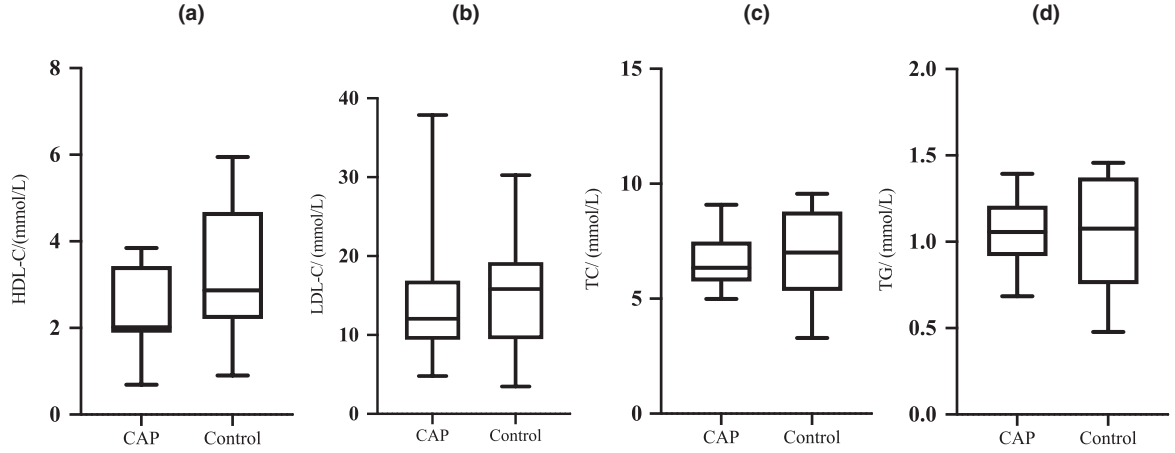

FIGURE 4 No significant difference was found in serum levels of either HDL-C (a), LDL-C (b), TC (c), or TG (d) between CAP and control group ($n = 8$ in each group). (* means $p < .05$).

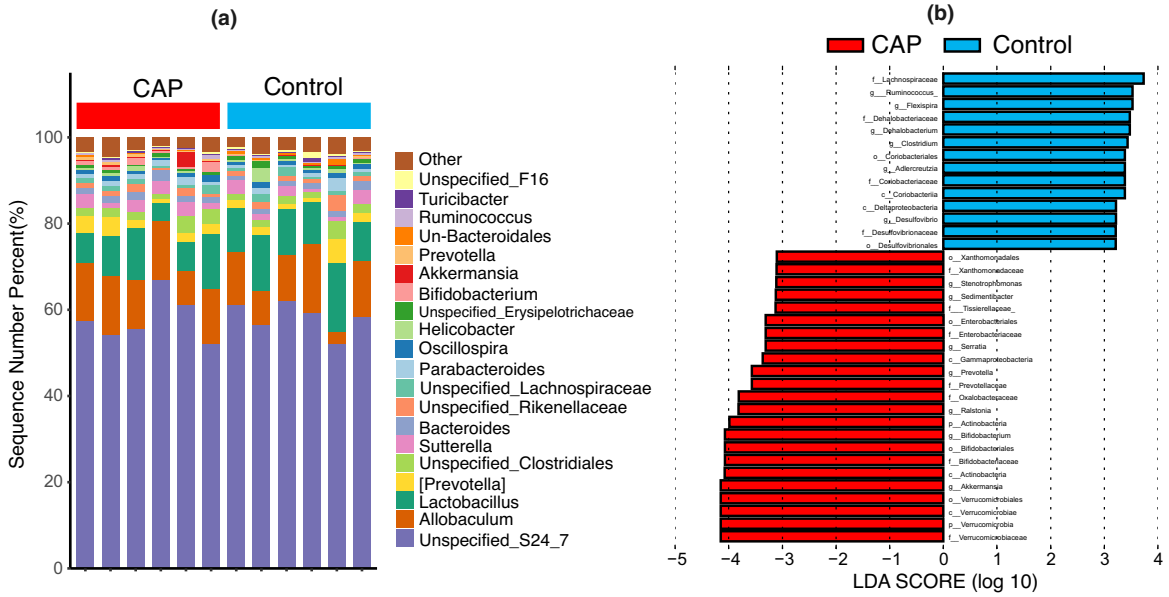

FIGURE 5 Comparison of the gut microbiota between CAP and control group by 16S rRNA gene sequencing. The bar chart shows the percentage of the top 20 most abundant gut microbiota in the two groups of mice (a). Linear discriminant analysis effect size (LEfSe) method was performed to compare taxa between the CAP and control groups (b). The bar plot lists the significantly different taxa ($p < .05$) based on effect size (LDA score (log 10) > ± 2).

to their compositional structure and generates PCoA (distance matrix calculated by Bray-Curtis distance) revealed the spatial separation of samples with different colours indicating groups (Figure 6d). Axis1 was the most contributing axis, accounting for 41.7% of the variance found in the microbiota, and axis2 explained 20.8% of the inter-sample variation (Figure 6d). The CAP and Control groups could be clearly distinguished by the microbial community ($p = .003$ in the PERMANOVA test). To explore whether the gut microbiota alteration correlated with exacerbation of atherosclerosis in the CAP group, a correlation analysis was performed between the percentage of atherosclerotic lesions and the relative abundance of gut microbiota at the phylum level. The results revealed that an increase in relative abundance of Firmicutes, Chloroflexi and Cyanobacteria together with a decrease in Bacteroidetes correlated to progress of atherosclerosis ($p < .05$; Figure 6e).

DISCUSSION

Epidemiological evidence suggests that CAP is associated with the development of atherosclerosis, but association does not always imply causality (Jimenez-Sanchez et al., 2020). There is a gap in the causality

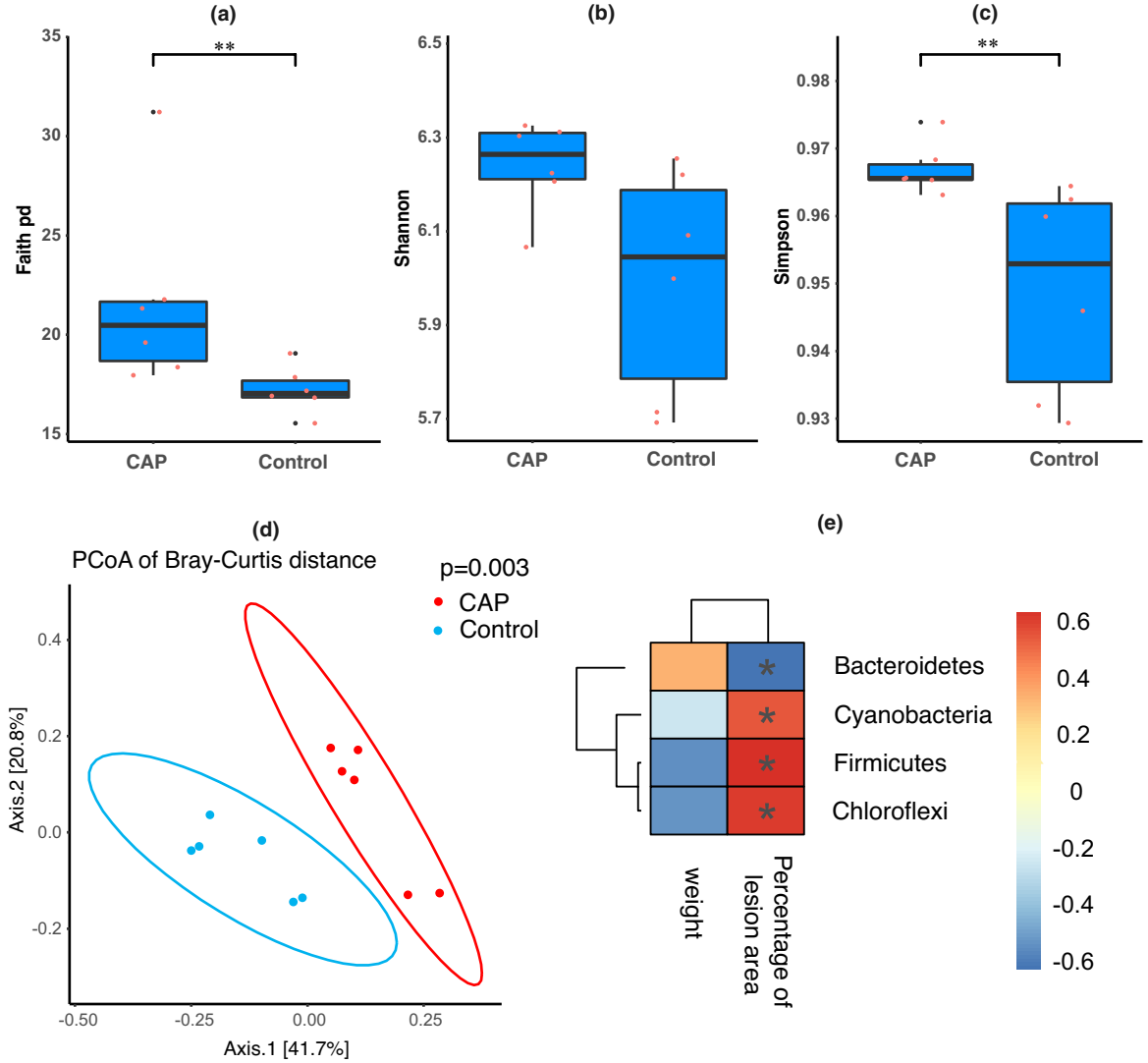

FIGURE 6 Data analysis of the diversity and distribution of gut microbiota in apoE$^{-/-}$ mice after dental infection with *P. gingivalis*. Alpha diversity was measured by Faith's phylogenetic diversity (a), Shannon index (b), and Simpson index (c). (** means $p < .01$) CAP group (red dots) and control group (blue dots) samples are each combined into a cluster in principal coordinate analysis (PCoA) of Bray-Curtis distance between sample diversity ($p = .003$) (d). The significant difference was found in Spearman's rank correlation between CAP and control groups using mouse body weight and percentage of aortic arch lesion area as environmental factors at the phylum level in the heatmap of co-occurrence analysis (e). ($p < .05$).

relationship between CAP and atherosclerosis, and animal studies are the key to investigating the role of CAP as a risk factor of atherosclerosis. Rabbits, pigs, and non-human primates are used for atherosclerosis research; each animal model has its advantages and disadvantages (Getz & Reardon, 2012). Mice have relatively low maintenance costs, but they are resistant to atherosclerosis in nature; genetic mouse models were created in the 1990s (Ishibashi et al., 1994; Nakashima et al., 1994). ApoE$^{-/-}$ and LDLr$^{-/-}$ mice are the most commonly used models for atherosclerosis research (Getz & Reardon, 2015). ApoE$^{-/-}$ mouse can form plaques on a chow diet or a high-fat/cholesterol diet, but LDLr$^{-/-}$ mice need a high-fat/cholesterol diet (Getz & Reardon, 2016). ApoE$^{-/-}$ mice were chosen and fed a normal diet to avoid the effects of high-fat diet on gut microbiota and atherosclerosis.

To determine the consistency of the experiment, 5-week-old apoE$^{-/-}$ male mice with a weight of 19 ± 2 g were used. After a week of adaptive feeding, the mice were randomly divided into the CAP group and Control group. FG 1/4 and Tc-21EF were used to explore the first and second molars of the bilateral maxillae. The condition of the exposure is shown in Figure 1a–b. The shape of the exposure facilitated the placement of cotton wool and the restoration of teeth with resin. The weight gain percentage and final weight of the two groups of mice were similar (Figure 1c), which suggests that the physical condition of

the CAP group was not affected by the surgery (Wang & Stashenko, 1991) and that the CAP group probably did not experience pain. Because of the comparison between this study and other studies using the CAP model, the monitoring data showed that apoE$^{-/-}$ mice can be used to study CAP and atherosclerosis.

Using micro-CT to study CAP is a good option, but there is no consistent protocol for analysing CAP in rodents (Kalatzis-Sousa et al., 2017). Parameters found in similar work was used for analysing CAP in rodents (Chen et al., 2019). The results of the micro-CT revealed that *P. gingivalis* dental infection after pulp exposure induced CAP, with PALs found in 98.2% of the molars. PALs were found in 92.8% of mice with all four molars. Compared with the CAP established by exposure of the four first molars (Berlin-Broner et al., 2020), the probability of PALs found in four molars was 27.7%. The low effectiveness of establishing CAP may be one of the reasons why atherosclerosis has not worsened. Another reason may be the absence of introduced foreign pathogens (natural infection of the exposed dental pulp by endogenous oral flora). In another study that used *P. gingivalis* infection in the bilateral first molars to induce CAP in C57BL/6J mice, injury of the arterial endothelium was found, but not atherosclerotic lesions (Ao et al., 2014). The reason may be that wild-type mice are inherently resistant to atherosclerosis. In this study, gene knockout mice were used and pathogens introduced after pulp exposure to induce a novel mouse model, which allowed the causal relationship between CAP and atherosclerosis to be studied. The positive rate of PALs also illustrates the stability of the CAP model established by dental infection of *P. gingivalis*.

The reason for using the aortic arch instead of the entire aorta for Oil Red O staining is that lesions will initially develop in the aortic arch. The presence of sparse lesions in the thoracic and abdominal aorta may preclude the utility of lesion measurements in this region (Daugherty & Rateri, 2005). This is consistent with the distribution of atherosclerotic lesions in the apoE$^{-/-}$ mice fed with the chow diet. The percentage of Oil Red O-stained areas at the aortic arch was increased in the CAP group compared with that in the Control group, with a significant difference in independent sample *t*-test (CAP: 2.001% ± 0.27%, Control: 0.927% ± 0.22%, $p = .005$). This is similar to the significant increase in atherosclerotic lesion area in the aorta of LDLr$^{-/-}$ mice infected with oral *P. gingivalis*; the lesion area was twice as large as that in the Control group (Brown et al., 2015). The results suggest that root canal infection of *P. gingivalis* in apoE$^{-/-}$ mice is feasible to establish the CAP to induce atherosclerosis in apoE$^{-/-}$ mice is feasible, which can be used to study the causal relationship between atherosclerosis and CAP.

One of the purposes of this study is to analyse the changes in serum lipids after dental infection of *P. gingivalis*. Hyperlipidaemia is considered a risk factor for atherosclerosis (Beverly & Budoff, 2020). In a previous study, decreased serum level of HDL-C and increase level of LDL-C were observed in rats feed with high-fat diet (Gobalakrishnan et al., 2016). A high level of HDL-C can prevent the formation of atherosclerotic plaques, thus reducing the incidence of CVD. Conversely, a high level of LDL-C is associated with major complications of atherosclerosis, such as cerebrovascular disease, coronary artery disease, and peripheral vascular disease (Gobalakrishnan et al., 2016). But, no significant changes were found in the levels of either TC, TG, HDL-C, or LDL-C in the present study. This might be explained by the relatively small sample size in this experiment. Larger sample sizes need to be considered in future study designs.

At the genus level, *Porphyromonas* was not found in the gut microbiota of either group of mice in the bar plot of the top 20 most abundant genera and the LEfse (Figure 5a–b). This is inconsistent with the experiments with oral *P. gingivalis* in C57BL/6N mice. After 5 weeks gavage of *P. gingivalis*, the gut microbiota composition of the mice was altered and the population of Bacteroidales was significantly increased (Arimatsu et al., 2014). This suggests that the altered composition of the gut microbiota in the CAP group was not caused by oral *P. gingivalis*. LEfSe was applied to the microbiota data from the two groups and identified 37 differentially abundant taxa, *Akkermansia* was the most abundant in the CAP group, whilst *Ruminococcus* was the most abundant in the Control group (Figure 5b). A positive correlation was found between the relative abundance of Akkermansia and the level of TMAO in patients with retinal artery occlusion (Zysset-Burri et al., 2019). Elevated levels of *Akkermansia* may collaborate with TMAO to exacerbate atherosclerosis, and it would be interesting to study the metabolites in stool and serum in future experiments. It was demonstrated that CAP increased the alpha diversity of the gut microbiota. Similar to the present results, oral infection with *P. gingivalis* increased the diversity of oral microbiota and the overgrowth of commensal species in the oral and intestinal microbiota (Simas et al., 2021). Given that PCoA and hierarchical clustering are unsupervised methods, they are suitable for this study. This study is the first to compare the changes in the gut microbiome of apoE$^{-/-}$ mice in response to CAP treatment, and 62.5% of the total variance in the sample was explained by the two main axes. As expected, the CAP and Control groups are clearly distinguished by the microbial community ($p = .003$ in the PERMANOVA test). This study explored whether the gut microbiota has any association with atherosclerosis in the CAP groups. The

results indicated that CAP had a significant effect on community composition (Figure 6d). Thus, the gut microbiota dysregulation induced by CAP may be related to atherosclerosis. These unique community profiles are associated with differences in percentages of lesion area. At the phylum level, the increase in members of Firmicutes, Chloroflexi and Cyanobacteria, and a decrease in Bacteroidetes are positively correlated with the lesion area of atherosclerosis (Figure 6e). The results demonstrate that the percentage of atherosclerotic lesion extent correlates with an increase in Firmicutes and a decrease in Bacteroidetes, which is similar to the altered gut microbiota in high-fat diet-induced apoE$^{-/-}$ mice, leading to atherosclerosis (Chan et al., 2016; Rom et al., 2017). However, this is in contrast to the results of apoE$^{-/-}$ mice infected with oral *P. gingivalis* and fed on a high-fat diet (Kramer et al., 2017), which revealed a decrease in *Firmicutes* and an increase in *Bacteroidetes*. This may be due to the direct oral administration of *P. gingivalis* (phylum Bacteroidetes), resulting in a relative increase in Bacteroidetes. It also implies that periodontitis and apical periodontitis, although the same oral infection, may affect the gut microbiota through different pathways. In future studies, it would be interesting to perform faecal microbial transplantation from CAP mice to unoperated mice to verify the causal relationship between altered gut microbiome and atherosclerosis.

CONCLUSION

This study is the first to use an apoE$^{-/-}$ mouse model to investigate the effect of CAP on atherosclerosis. This model can be used to study the relationship between the two diseases and the altered gut microbiota diversity during this process whilst avoiding the effect of a high-fat diet on the gut microbiota. In this study, dental infection of *P. gingivalis*-induced CAP with a high success rate, which aggravates the degree of atherosclerosis. Interestingly, the gut microbiota alpha diversity is increased in the CAP group (Fig. Graphical abstract). The CAP and Control groups are clearly distinguished by the microbial community. This study could be considered as a basis for future studies to investigate the alterations in serum inflammatory markers induced by CAP and also to verify the role of gut microbiota in the atherosclerotic process by faecal microbiota transplantation.

ACKNOWLEDGEMENTS

The authors thank Servier Medical Art (smart.servier.com) for providing the elements for the images in the graphic abstract.

CONFLICT OF INTEREST

The authors have stated explicitly that there are no conflicts of interest in connection with this article.

ETHICAL APPROVAL

The study has been reviewed and approved by Animal Care and Use Committee of Fujian Medical University (protocol number 2020-0041).

AUTHOR CONTRIBUTIONS

Guowu Gan: study concept and design, performed the animal experiment, generation of figures, writing of the original manuscript. Beibei Lu: performed the animal experiment, data acquisition, review of manuscript. Ren Zhang: performed the animal experiment, data acquisition. Yufang Luo: performed the bacteria experiment, literature search. Shuai Chen: design of animal experimental models. Huaxiang Lei: performed the image analyses. Yijun Li: operation of experimental instrument. Zhiyu Cai: performed statistical analysis, study concept and design. Xiaojing Huang: study concept and design, data acquisition and analysis, editing and review of manuscript.

ORCID

Guowu Gan https://orcid.org/0000-0002-3189-9915
Beibei Lu https://orcid.org/0000-0002-7588-1979
Shuai Chen https://orcid.org/0000-0002-6619-2485
Huaxiang Lei https://orcid.org/0000-0002-7261-7128
Yijun Li https://orcid.org/0000-0003-0602-5041

REFERENCES

Aimetti, M., Romano, F. & Nessi, F. (2007) Microbiologic analysis of periodontal pockets and carotid atheromatous plaques in advanced chronic periodontitis patients. *Journal of Periodontology*, 78, 1718–1723.

An, G.K., Morse, D.E., Kunin, M., Goldberger, R.S. & Psoter, W.J. (2016) Association of radiographically diagnosed apical periodontitis and cardiovascular disease: a hospital records-based study. *Journal of Endodontics*, 42, 916–920.

Ao, M., Miyauchi, M., Inubushi, T., Kitagawa, M., Furusho, H., Ando, T. et al. (2014) Infection with *Porphyromonas gingivalis* exacerbates endothelial injury in obese mice. *PLoS One*, 9, e110519.

Arimatsu, K., Yamada, H., Miyazawa, H., Minagawa, T., Nakajima, M., Ryder, M.I. et al. (2014) Oral pathobiont induces systemic inflammation and metabolic changes associated with alteration of gut microbiota. *Scientific Reports*, 4, 4828.

Berlin-Broner, Y., Alexiou, M., Levin, L. & Febbraio, M. (2020) Characterization of a mouse model to study the relationship between apical periodontitis and atherosclerosis. *International Endodontic Journal*, 53, 812–823.

Berlin-Broner, Y., Febbraio, M. & Levin, L. (2017) Apical periodontitis and atherosclerosis: is there a link? Review of the literature and potential mechanism of linkage. *Quintessence International*, 48, 527–534.

Beverly, J.K. & Budoff, M.J. (2020) Atherosclerosis: pathophysiology of insulin resistance, hyperglycemia, hyperlipidemia, and inflammation. *Journal of Diabetes*, 12, 102–104.

Bokulich, N.A., Kaehler, B.D., Rideout, J.R., Dillon, M., Bolyen, E., Knight, R. et al. (2018) Optimizing taxonomic classification of marker-gene amplicon sequences with QIIME 2's q2-feature-classifier plugin. *Microbiome*, 6, 90.

Brandsma, E., Kloosterhuis, N.J., Koster, M., Dekker, D.C., Gijbels, M.J.J., van der Velden, S. et al. (2019) A proinflammatory gut microbiota increases systemic inflammation and accelerates atherosclerosis. *Circulation Research*, 124, 94–100.

Brown, P.M., Kennedy, D.J., Morton, R.E. & Febbraio, M. (2015) CD36/SR-B2-TLR2 dependent pathways enhance *Porphyromonas gingivalis* mediated atherosclerosis in the Ldlr KO mouse model. *PLoS One*, 10, e0125126.

Bui, F.Q., Almeida-da-Silva, C.L.C., Huynh, B., Trinh, A., Liu, J., Woodward, J. et al. (2019) Association between periodontal pathogens and systemic disease. *Biomedical Journal*, 42, 27–35.

Callahan, B.J., McMurdie, P.J., Rosen, M.J., Han, A.W., Johnson, A.J. & Holmes, S.P. (2016) DADA2: High-resolution sample inference from Illumina amplicon data. *Nature Methods*, 13, 581–583.

Campbell, L.A. & Rosenfeld, M.E. (2015) Infection and atherosclerosis development. *Archives of Medical Research*, 46, 339–350.

Centa, M., Ketelhuth, D.F.J., Malin, S. & Gistera, A. (2019) Quantification of atherosclerosis in mice. *Journal of Visualized Experiments*, 59828.

Chan, Y.K., Brar, M.S., Kirjavainen, P.V., Chen, Y., Peng, J., Li, D. et al. (2016) High fat diet induced atherosclerosis is accompanied with low colonic bacterial diversity and altered abundances that correlates with plaque size, plasma A-FABP and cholesterol: a pilot study of high fat diet and its intervention with *Lactobacillus rhamnosus* GG (LGG) or telmisartan in ApoE(−/−) mice. *BMC Microbiology*, 16, 264.

Chauhan, N., Mittal, S., Tewari, S., Sen, J. & Laller, K. (2019) Association of apical periodontitis with cardiovascular disease via noninvasive assessment of endothelial function and subclinical atherosclerosis. *Journal of Endodontics*, 45, 681–690.

Chen, S., Lei, H., Luo, Y., Jiang, S., Zhang, M., Lv, H. et al. (2019) Micro-CT analysis of chronic apical periodontitis induced by several specific pathogens. *International Endodontic Journal*, 52, 1028–1039.

Conti, L.C., Segura-Egea, J.J., Cardoso, C.B.M., Benetti, F., Azuma, M.M., Oliveira, P.H.C. et al. (2020) Relationship between apical periodontitis and atherosclerosis in rats: lipid profile and histological study. *International Endodontic Journal*, 53, 1387–1397.

Daugherty, A. & Rateri, D.L. (2005) Development of experimental designs for atherosclerosis studies in mice. *Methods*, 36, 129–138.

Daugherty, A., Tall, A.R., Daemen, M., Falk, E., Fisher, E.A., García-Cardeña, G et al. (2017) Recommendation on design, execution, and reporting of animal atherosclerosis studies: a scientific statement from the American Heart Association. *Arteriosclerosis, Thrombosis, and Vascular Biology*, 37, e131–e157.

Getz, G.S. & Reardon, C.A. (2012) Animal models of atherosclerosis. *Arteriosclerosis, Thrombosis, and Vascular Biology*, 32, 1104–1115.

Getz, G.S. & Reardon, C.A. (2015) Use of mouse models in atherosclerosis research. *Methods in Molecular Biology*, 1339, 1–16.

Getz, G.S. & Reardon, C.A. (2016) Do the Apoe−/− and Ldlr−/− mice yield the same insight on atherogenesis? *Arteriosclerosis, Thrombosis, and Vascular Biology*, 36, 1734–1741.

Gibson, F.C., Hong, C., Chou, H.-H., Yumoto, H., Chen, J., Lien, E. et al. (2004) Innate immune recognition of invasive bacteria accelerates atherosclerosis in apolipoprotein E-deficient mice. *Circulation*, 109, 2801–2806.

Gistera, A. & Hansson, G.K. (2017) The immunology of atherosclerosis. *Nature Reviews Nephrology*, 13, 368–380.

Gobalakrishnan, S., Asirvatham, S.S. & Janarthanam, V. (2016) Effect of silybin on lipid profile in hypercholesterolaemic rats. *Journal of Clinical and Diagnostic Research*, 10, FF01-05.

González-Navarro, B., Segura-Egea, J.J., Estrugo-Devesa, A., Pintó-Sala, X., Jane-Salas, E., Jiménez-Sánchez, M.C. et al. (2020) Relationship between apical periodontitis and metabolic syndrome and cardiovascular events: a cross-sectional study. *Journal of Clinical Medicine*, 9,3205.

Ishibashi, S., Goldstein, J.L., Brown, M.S., Herz, J. & Burns, D.K. (1994) Massive xanthomatosis and atherosclerosis in cholesterol-fed low density lipoprotein receptor-negative mice. *Journal of Clinical Investigation*, 93, 1885–1893.

Jimenez-Sanchez, M.C., Cabanillas-Balsera, D., Areal-Quecuty, V., Velasco-Ortega, E., Martin-Gonzalez, J. & Segura-Egea, J.J. (2020) Cardiovascular diseases and apical periodontitis: association not always implies causality. *Medicina Oral Patologia Oral Y Cirugia Bucal*, 25, e652–e659.

Kalatzis-Sousa, N.G., Spin-Neto, R., Wenzel, A., Tanomaru-Filho, M. & Faria, G. (2017) Use of micro-computed tomography for the assessment of periapical lesions in small rodents: a systematic review. *International Endodontic Journal*, 50, 352–366.

Koeth, R.A., Wang, Z., Levison, B.S., Buffa, J.A., Org, E., Sheehy, B.T. et al. (2013) Intestinal microbiota metabolism of L-carnitine, a nutrient in red meat, promotes atherosclerosis. *Nature Medicine*, 19, 576–585.

Koren, O., Spor, A., Felin, J., Fak, F., Stombaugh, J., Tremaroli, V. et al. (2011) Human oral, gut, and plaque microbiota in patients with atherosclerosis. *Proceedings of the National Academy of Sciences of the United States of America*, 108(Suppl. 1), 4592–4598.

Kramer, C.D., Simas, A.M., He, X., Ingalls, R.R., Weinberg, E.O. & Genco, C.A. (2017) Distinct roles for dietary lipids and *Porphyromonas gingivalis* infection on atherosclerosis progression and the gut microbiota. *Anaerobe*, 45, 19–30.

López-López, J., Jané-Salas, E., Estrugo-Devesa, A., Castellanos-Cosano, L., Martín-González, J., Velasco-Ortega, E. et al. (2012) Frequency and distribution of root-filled teeth and apical periodontitis in an adult population of Barcelona, Spain. *International Dental Journal*, 62, 40–46.

Love, M.I., Huber, W. & Anders, S. (2014) Moderated estimation of fold change and dispersion for RNA-seq data with DESeq2. *Genome Biology*, 15, 550.

Mandal, S., Van Treuren, W., White, R.A., Eggesbo, M., Knight, R. & Peddada, S.D. (2015) Analysis of composition of microbiomes: a novel method for studying microbial composition. *Microbial Ecology in Health and Disease*, 26, 27663.

Nagendrababu, V., Kishen, A., Murray, P.E., Nekoofar, M.H., Figueiredo, J.A.P., Priya, E. et al. (2021) PRIASE 2021 guidelines for reporting animal studies in Endodontology: a consensus-based development. *International Endodontic Journal*, 54, 848–857.

Nakashima, Y., Plump, A.S., Raines, E.W., Breslow, J.L. & Ross, R. (1994) ApoE-deficient mice develop lesions of all phases of atherosclerosis throughout the arterial tree. *Arteriosclerosis Thrombosis*, 14, 133–140.

Persoon, I.F. & Ozok, A.R. (2017) Definitions and epidemiology of endodontic infections. *Current Oral Health Reports*, 4, 278–285.

Petersen, J., Glaßl, E.-M., Nasseri, P., Crismani, A., Luger, A.K., Schoenherr, E. et al. (2014) The association of chronic apical periodontitis and endodontic therapy with atherosclerosis. *Clinical Oral Investigations*, 18, 1813–1823.

Rom, O., Korach-Rechtman, H., Hayek, T., Danin-Poleg, Y., Bar, H., Kashi, Y. et al. (2017) Acrolein increases macrophage atherogenicity in association with gut microbiota remodeling in atherosclerotic mice: protective role for the polyphenol-rich pomegranate juice. *Archives of Toxicology*, 91, 1709–1725.

Segata, N., Izard, J., Waldron, L., Gevers, D., Miropolsky, L., Garrett, W.S. et al. (2011) Metagenomic biomarker discovery and explanation. *Genome Biology*, 12, R60.

Segura-Egea, J.J., Martin-Gonzalez, J. & Castellanos-Cosano, L. (2015) Endodontic medicine: connections between apical periodontitis and systemic diseases. *International Endodontic Journal*, 48, 933–951.

Shapiro, M.D. & Fazio, S. (2016) From lipids to inflammation: new approaches to reducing atherosclerotic risk. *Circulation Research*, 118, 732–749.

Simas, A.M., Kramer, C.D., Weinberg, E.O. & Genco, C.A. (2021) Oral infection with a periodontal pathogen alters oral and gut microbiomes. *Anaerobe*, 71, 102399.

Suh, J.S., Kim, S., Bostrom, K.I., Wang, C.Y., Kim, R.H. & Park, N.H. (2019) Periodontitis-induced systemic inflammation exacerbates atherosclerosis partly via endothelial-mesenchymal transition in mice. *International Journal of Oral Science*, 11, 21.

Sullivan, M., Gallagher, G. & Noonan, V. (2016) The root of the problem: occurrence of typical and atypical periapical pathoses. *Journal of the American Dental Association*, 147, 646–649.

Tang, W.H.W., Wang, Z., Levison, B.S., Koeth, R.A., Britt, E.B., Fu, X. et al. (2013) Intestinal microbial metabolism of phosphatidylcholine and cardiovascular risk. *New England Journal of Medicine*, 368, 1575–1584.

Tymchuk, C.N., Hartiala, J., Patel, P.I., Mehrabian, M. & Allayee, H. (2006) Nonconventional genetic risk factors for cardiovascular disease. *Current Atherosclerosis Reports*, 8, 184–192.

Vazquez-Baeza, Y., Pirrung, M., Gonzalez, A. & Knight, R. (2013) EMPeror: a tool for visualizing high-throughput microbial community data. *Gigascience*, 2, 16.

Wang, C.Y. & Stashenko, P. (1991) Kinetics of bone-resorbing activity in developing periapical lesions. *Journal of Dental Research*, 70, 1362–1366.

Wang, Z., Klipfell, E., Bennett, B.J., Koeth, R., Levison, B.S., DuGar, B. et al. (2011) Gut flora metabolism of phosphatidylcholine promotes cardiovascular disease. *Nature*, 472, 57–63.

Yu, V.S., Messer, H.H., Yee, R. & Shen, L. (2012) Incidence and impact of painful exacerbations in a cohort with post-treatment persistent endodontic lesions. *Journal of Endodontics*, 38, 41–46.

Zhang, J., Huang, X., Lu, B., Zhang, C. & Cai, Z. (2016) Can apical periodontitis affect serum levels of CRP, IL-2, and IL-6 as well as induce pathological changes in remote organs? *Clinical Oral Investigations*, 20, 1617–1624.

Zysset-Burri, D.C., Keller, I., Berger, L.E., Neyer, P.J., Steuer, C., Wolf, S. et al. (2019) Retinal artery occlusion is associated with compositional and functional shifts in the gut microbiome and altered trimethylamine-N-oxide levels. *Scientific Reports*, 9, 15303.

How to cite this article: Gan, G., Lu, B., Zhang, R., Luo, Y., Chen, S., Lei, H., et al. (2022) Chronic apical periodontitis exacerbates atherosclerosis in apolipoprotein E-deficient mice and leads to changes in the diversity of gut microbiota. *International Endodontic Journal*, 55, 152–163. https://doi.org/10.1111/iej.13655